

## Investigating collective effects in small collision systems using PYTHIA8 and EPOS4 simulations

A. DANU<sup>(1)</sup>, C. BRANDIBUR<sup>(1)</sup>, A. DOBRIN<sup>(1)</sup>, A. MANEA<sup>(1)(4)(\*)</sup>, S. BASU<sup>(2)</sup>,  
V. GONZALEZ<sup>(3)</sup> and C. PRUNEAU<sup>(3)</sup>

<sup>(1)</sup> *Institute of Space Science, INFLPR subsidiary - 409 Atomistilor Street, Magurele, Ilfov, 077125, Romania*

<sup>(2)</sup> *Lund University, Department of Physics, Division of Particle Physics - Box 118, SE-221 00, Lund, Sweden*

<sup>(3)</sup> *Department of Physics and Astronomy, Wayne State University - Detroit, 48201, MI, USA*

<sup>(4)</sup> *University of Bucharest, Faculty of Physics - Bucharest, Magurele, 077125, Romania*

received 23 July 2024

**Summary.** — Measurements of azimuthal angular correlations of inclusive and identified particles from EPOS4 and PYTHIA8 event generators are used to study the unexpected collective behavior observed in small collision systems. In particular, anisotropic flow coefficients measured using two- and four-particle correlations and balance functions are reported in pp collisions at  $\sqrt{s} = 13.6$  TeV. The second-order Fourier coefficient of  $\pi^\pm$ ,  $K^\pm$ ,  $p+\bar{p}$ ,  $\Lambda+\bar{\Lambda}$ ,  $K_S^0$ , and  $\Xi^-+\bar{\Xi}^+$  obtained using the scalar product method exhibits a mass ordering at low transverse momentum when a pseudorapidity gap of  $|\Delta\eta| > 2$  is used, being more pronounced for EPOS4. The second harmonic two-particle cumulants of inclusive charged particles decrease with charged-particle multiplicity and depend weakly on  $|\Delta\eta|$ , while the second harmonic four-particle cumulants are consistent with zero. The balance functions show different responses, being influenced by the different charge production mechanisms.

### 1. – Introduction

Measurements of two- and multi-particle azimuthal correlations in small collision systems, such as proton–proton (pp) and proton–lead (p–Pb) at the Large Hadron Collider, revealed an unexpected collective behaviour similar to the one observed in heavy-ion collisions. The two-particle correlation function *versus* the difference in azimuth,  $\Delta\varphi$ , and pseudorapidity,  $\Delta\eta$ , shows a ridge in the near-side region ( $\Delta\varphi \approx 0$  over a wide range in  $\Delta\eta$ ) [1,2]. Multi-particle correlations indicate that this ridge has a collective origin [3,4]. In addition, the  $v_n$  coefficients of identified particles in a Fourier decomposition of the

(\*) E-mail: alexandrumanea@spacescience.ro

particle azimuthal distribution [5] exhibit a mass ordering at low transverse momentum,  $p_T$ , and a crossing of baryons and mesons at intermediate  $p_T$  [4, 6].

Two Monte Carlo event generators, PYTHIA8 [7] and EPOS4 [8], are used to investigate the origin of collectivity in pp collisions at  $\sqrt{s} = 13.6$  TeV through two- and multi-particle azimuthal correlations of inclusive and identified particles and charge balance functions. A “core-corona” picture coupled to a hadronic afterburner is implemented in EPOS4 where hard processes (*e.g.*, jets) are handled using strings in the “corona” region and the soft processes follow a hydrodynamic evolution in the “core” part. PYTHIA8 uses string fragmentation and implements new models that give rise to collective effects, *e.g.*, rope hadronization [9]. This new mechanism allows strings to interact coherently and increases the effective color-field strength thereby enhancing the probability of creating heavier particles. Two PYTHIA configurations (rope hadronization and Monash tune [10]) are used in pp simulations.

## 2. – Observables

The second order Fourier coefficient  $v_2$  of  $\pi^\pm$ ,  $K^\pm$ ,  $p+\bar{p}$ ,  $\Lambda+\bar{\Lambda}$ ,  $K_S^0$ , and  $\Xi^-+\bar{\Xi}^+$  is computed using the scalar product method [11]

$$(1) \quad v_2\{\text{SP}\} = \frac{\langle \mathbf{u}_{2,k} \mathbf{Q}_2^* / M \rangle}{\sqrt{\langle \mathbf{Q}_2^a \mathbf{Q}_2^{b*} / (M^a M^b) \rangle}},$$

where  $\mathbf{u}_{2,k} = \exp(i2\varphi_k)$  is the unit flow vector of the particle  $k$  with azimuthal angle  $\varphi_k$ ,  $\mathbf{Q}_2^* = \sum_j \exp(i2\varphi_j)$  is the event flow vector, and  $M$  is the event multiplicity. Each event is divided into two sub-events represented by  $Q_2^a$  and  $Q_2^b$  determined by tracks selected in a specific pseudorapidity interval and the associated multiplicities  $M^a$  and  $M^b$ . The angle brackets represent an average over all events and particles and  $*$  denotes the complex conjugate. To suppress contributions from nonflow (*i.e.*, short-range correlations, such as those due to jets and resonances) various  $|\Delta\eta|$  gaps are employed.

In the context of the cumulant method [12, 13], the second order two- and four-particle cumulants of unidentified charged particles are calculated as

$$(2) \quad c_2\{2\} = \langle\langle 2 \rangle\rangle,$$

$$(3) \quad c_2\{4\} = \langle\langle 4 \rangle\rangle - 2 \cdot \langle\langle 2 \rangle\rangle.$$

Charge balance function, which probe the time evolution of particle production in heavy-ion collisions [14], are computed based on differential cumulants defined as [15]

$$(4) \quad B^{\alpha\bar{\beta}}(\Delta y|y_0) = \frac{1}{\langle N_1^{\bar{\beta}} \rangle} \sum_{\bar{y}} [C_2^{\alpha\bar{\beta}}(\bar{y}, \Delta y) - C_2^{\bar{\alpha}\bar{\beta}}(\bar{y}, \Delta y)],$$

where cumulants are computed as  $C_2^{\alpha\bar{\beta}}(y_1, y_2) = \rho_2^{\alpha\bar{\beta}}(y_1, y_2) - \rho_1^\alpha(y_1)\rho_1^{\bar{\beta}}(y_2)$  in which  $\rho_2^{\alpha\bar{\beta}}(y_1, y_2)$  and  $\rho_1^\alpha(y)$  are pair and single particle densities, respectively, for particle species  $\alpha$  and  $\bar{\beta}$ . Labels  $\bar{\alpha}$  and  $\bar{\beta}$  represent anti-particles of species  $\alpha$  and  $\beta$ , respectively, whereas  $\langle N_1^{\bar{\beta}} \rangle$  is the average number of particles of type  $\bar{\beta}$  per event.

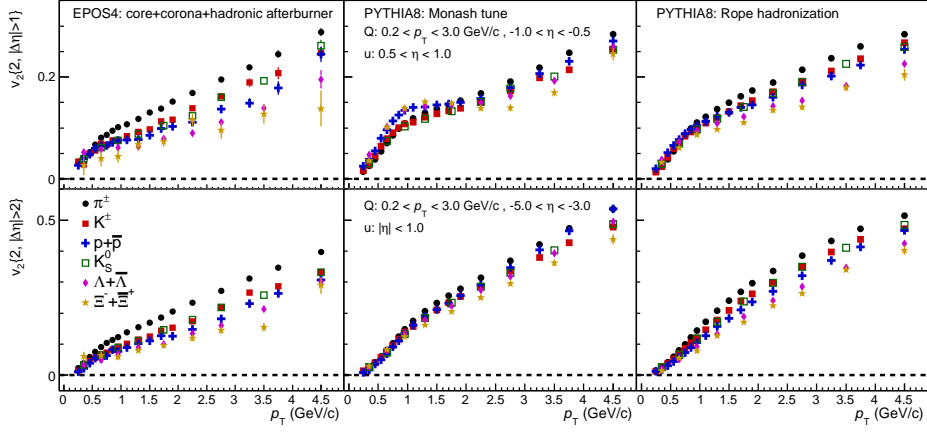


Fig. 1. – The  $p_T$ -differential  $v_2$  of  $\pi^\pm$ ,  $K^\pm$ ,  $p+\bar{p}$ ,  $\Lambda+\bar{\Lambda}$ ,  $K_S^0$ , and  $\Xi^-+\bar{\Xi}^+$  for  $|\Delta\eta| > 1$  (top) and  $|\Delta\eta| > 2$  (bottom) from different EPOS4 and PYTHIA8 configurations of pp collisions at  $\sqrt{s} = 13.6$  TeV.

Integrals of the general balance functions are computed according to

$$(5) \quad I^{\alpha\bar{\beta}} \equiv \frac{\langle N_2^{\alpha\bar{\beta}} \rangle}{\langle N_1^{\bar{\beta}} \rangle} - \frac{\langle N_2^{\bar{\alpha}\beta} \rangle}{\langle N_1^{\alpha} \rangle} - (\langle N_1^{\alpha} \rangle - \langle N_1^{\bar{\alpha}} \rangle),$$

in order to account for the non-vanishing net charge of pp collisions. By construction,  $I^{\alpha\bar{\beta}}$  converges to unity for a full rapidity ( $y$ ),  $\varphi$ , and  $p_T$  acceptance but amounts to a fraction of unity for narrow acceptances in  $y$  and  $p_T$  encountered experimentally.

### 3. – Results

Figure 1 presents the  $p_T$ -differential  $v_2$  of  $\pi^\pm$ ,  $K^\pm$ ,  $p+\bar{p}$ ,  $\Lambda+\bar{\Lambda}$ ,  $K_S^0$ , and  $\Xi^-+\bar{\Xi}^+$  for  $|\Delta\eta| > 1$  (top) and  $|\Delta\eta| > 2$  (bottom) calculated with EPOS4 and PYTHIA8 simulations. A mass ordering (*i.e.*, heavier particles have a smaller  $v_2$  than lighter particles at the same  $p_T$ ) is observed at low transverse momenta for both  $|\Delta\eta|$  gaps for EPOS4, being more pronounced for  $|\Delta\eta| > 2$  gap. For PYTHIA8, the mass ordering is broken for  $|\Delta\eta| > 1$  gap which is recovered when increasing the gap size to  $|\Delta\eta| > 2$ . For  $p_T > 2$  GeV/c, no crossing between baryon and meson  $v_2$  and no particle type grouping are present in either cases.

The second order two- ( $c_2\{2\}$ ) and four-particle ( $c_2\{4\}$ ) cumulants of unidentified charged particles are presented as a function of charged-particle multiplicity  $N_{\text{ch}}$  in the top and bottom panels of fig. 2, respectively. The trends are qualitatively similar in all configurations although there are quantitative differences between EPOS4 and PYTHIA8 results. The  $c_2\{2\}$  is positive, depends weakly on the  $|\Delta\eta|$  gap that suppresses nonflow contributions, and decreases with  $N_{\text{ch}}$  and  $|\Delta\eta|$ . The  $c_2\{4\}$  depends on multiplicity for  $N_{\text{ch}} < 50$ , while it is consistent with zero at high multiplicities. Employing an  $|\Delta\eta|$  gap, the  $c_2\{4\}$  is consistent with zero over the entire multiplicity range. This behaviour is expected for Gaussian fluctuations of the sources.

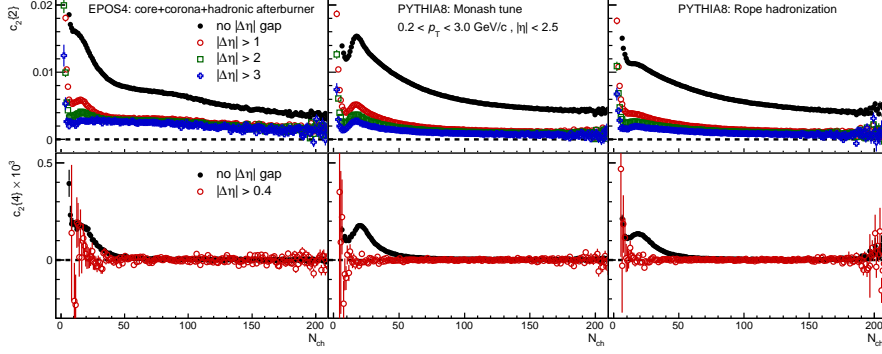


Fig. 2. –  $c_2\{2\}$  (top) and  $c_2\{4\}$  (bottom) for different  $|\Delta\eta|$  gaps as a function of charged-particle multiplicity from different EPOS4 and PYTHIA8 configurations of pp collisions at  $\sqrt{s} = 13.6$  TeV.

Figure 3 presents the charge balance functions of unidentified charged particles from different EPOS4 and PYTHIA8 configurations. The near-side peak is narrower for EPOS4 compared with PYTHIA8 results in both  $\Delta\eta$  and  $\Delta\varphi$  regions. Differences are also observed on the away-side between EPOS4 and PYTHIA8 and between the two PYTHIA configurations. These differences are propagated to the integrals of the balance functions reported in table I.

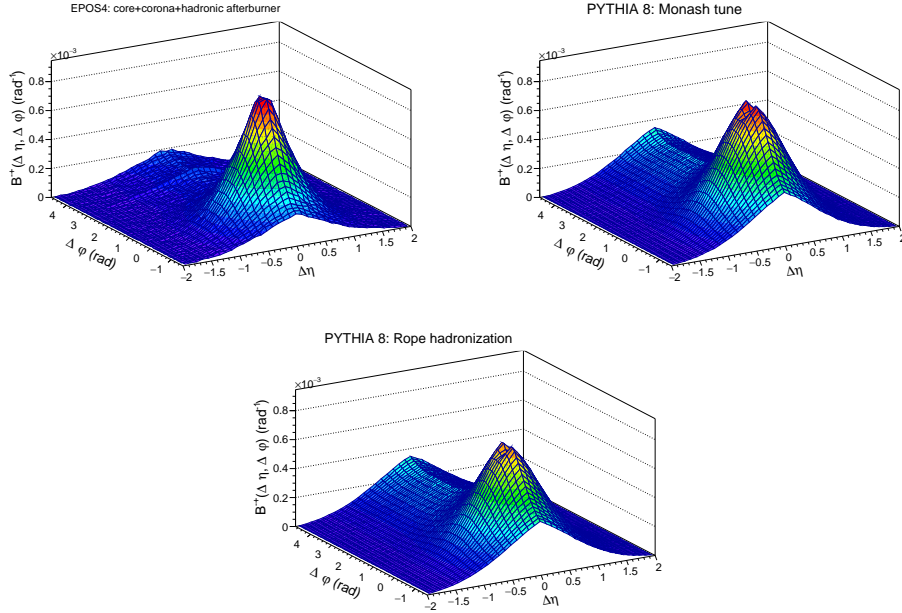


Fig. 3. – Charge balance functions  $B^{+-}$  of unidentified charged particles evaluated for  $0.2 < p_T < 2.0$  GeV/c within  $|\eta| < 1$  from different EPOS4 and PYTHIA8 configurations of pp collisions at  $\sqrt{s} = 13.6$  TeV.

TABLE I. – Integrals of the balance functions ( $B^{+-}$ ,  $B^{-+}$ ) of unidentified charged particles evaluated for  $0.2 < p_T < 2.0$  GeV/c within  $|\eta| < 1$  from different EPOS4 and PYTHIA8 configurations.

Balance function	EPOS4	PYTHIA8 (Monash)	PYTHIA8 (Rope)
$B^{+-}$	0.344	0.490	0.469
$B^{-+}$	0.336	0.486	0.474

#### 4. – Summary

Two- and multi-particle azimuthal correlations and charge balance functions are extracted from PYTHIA8 and EPOS4 simulations of pp collisions at  $\sqrt{s} = 13.6$  TeV. While  $c_2\{2\}$  is positive and decreases with charged-particle multiplicity, the  $c_2\{4\}$  is consistent with zero. These observations are qualitatively similar for all configurations. The  $v_2$  of various particle species is mass-ordered when an  $|\Delta\eta| > 2$  gap is employed to suppress nonflow contributions, being more pronounced for EPOS4. The balance functions show different responses and can be used to constrain the particle production mechanism.

\* \* \*

This work was supported in part by a grant from the Romanian Ministry of Research, Innovation and Digitization, CNCS – UEFISCDI, project number PN-III-P4-PCE-2021-0390, within PNCDI III, and by the United States Department of Energy, Office of Nuclear Physics (DOE NP), United States of America under Grant No. DE-FOA-0001664 and U.S. Department of Energy Office of Science under contract number DE-SC0013391. SB also acknowledges the support of the Swedish Research Council (VR).

#### REFERENCES

- [1] KHACHATRYAN V. *et al.*, *JHEP*, **09** (2010) 091.
- [2] ABELEV B. *et al.*, *Phys. Lett. B*, **719** (2013) 29.
- [3] ABELEV B. *et al.*, *Phys. Rev. C*, **90** (2014) 054901.
- [4] KHACHATRYAN V. *et al.*, *Phys. Lett. B*, **765** (2017) 193.
- [5] VOLOSHIN S. and ZHANG Y., *Z. Phys. C*, **70** (1996) 665.
- [6] ABELEV B. B. *et al.*, *Phys. Lett. B*, **726** (2013) 164.
- [7] BIERLICH C. *et al.*, *SciPost Phys. Codebases*, **2022** (2022) 8.
- [8] WERNER K., *Phys. Rev. C*, **108** (2023) 064903.
- [9] BIERLICH C., GUSTAFSON G., LÖNNBLAD L. and TARASOV A., *JHEP*, **03** (2015) 148.
- [10] SKANDS P., CARRAZZA S. and ROJO J., *Eur. Phys. J. C*, **74** (2014) 3024.
- [11] ADLER C. *et al.*, *Phys. Rev. C*, **66** (2002) 034904.
- [12] BILANDZIC A., SNELLINGS R. and VOLOSHIN S., *Phys. Rev. C*, **83** (2011) 044913.
- [13] JIA J., ZHOU M. and TRZUPEK A., *Phys. Rev. C*, **96** (2017) 034906.
- [14] BASS S. A., DANIELEWICZ P. and PRATT S., *Phys. Rev. Lett.*, **85** (2000) 2689.
- [15] PRUNEAU C., GONZALEZ V., HANLEY B., MARIN A. and BASU S., arXiv:2209.10420 [hep-ph] (2022).